Applied Catalysis B: Environmental 90 (2009) 89–98

Contents lists available at ScienceDirect

Applied Catalysis B: Environmental

journal homepage: www.elsevier.com/locate/apcatb

Photocatalytic oxidation of 1,3-dichloro-2-propanol aqueous solutions with modified TiO_2 catalysts

Maria D. Nikolaki, Caterina N. Zerva, Constantine J. Philippopoulos *

Chemical Process Engineering Laboratory, Department of Chemical Engineering, National Technical University, 9 Heroon Polytechneiou Str., Zografou Campus, 157 80 Athens, Greece

ARTICLE INFO

Article history:
Received 5 September 2008
Received in revised form 11 February 2009
Accepted 19 February 2009
Available online 28 February 2009

Keywords:
1,3-Dichloro-2-propanol
TiO_2
Photocatalysis
Kinetic study

ABSTRACT

The photochemical and photocatalytic oxidation of 1,3-dichloro-2-propanol (1,3-DCP, 0.024 M) was performed in a batch reactor, at room temperature, using UV radiation (254 nm), H_2O_2 (0.081 M and 0.163 M) as oxidant, and TiO_2-based catalysts modified with platinum, cerium and iron (65 mg/L catalyst load). The profile of the oxidation of 1,3-DCP was followed by monitoring the target compound degradation, the total organic carbon removal and the chloride ion production and it was deduced that the addition of the catalysts enhances the mineralization process taking place during the oxidation with simultaneous 1,3-DCP conversion. Based on the oxidation intermediates detected a reaction pathway for the degradation of 1,3-DCP is proposed. Also, a seven-step reaction mechanism was proposed, according to which a total chlorinated intermediate was produced, that degraded further to chloroacetic, acetic and formic acids, while chloroacetic and acetic acids were mineralized with simultaneous production of formic acid. Finally, based on the proposed mechanism a kinetic analysis was conducted in order to calculate the respective rate constants and it was deduced that with the catalyst's addition, the direct mineralization of the chlorinated intermediate was enhanced increasing TOC removal, whereas formic acid was resistant to further degradation, posing an obstacle to the total mineralization of 1,3-DCP.

1. Introduction

Dichloropropanols constitute an important class of water pollutants because of their toxicity to living organisms and bioaccumulation. They are used in industries such as hard resin production, chlorination of water or fabrication of paper. In particular, 1,3-dichloro-2-propanol (1,3-DCP) is formed in the reaction of epichlorohydrin with chloride ions and belongs to the family of halohydrins that are used widely as reagents in chemical manufacture. Moreover, 1,3-DCP is carcinogenic, mutagenic and genotoxic, having a high risk factor for human and animal toxicity with regards to the environment [1] and according to EU directive 91/155/EEC, all formulations which contain more than 0.1% of DCP have to be labeled as toxic and carcinogenic [2]. Although little information is available on the photodegradation of 1,3-DCP [3,4], attention has been paid to its biodegradation [1,5–7] and on toxicity studies [8,9]. 1,3-DCP was selected due to its high volume production and use, potential for human exposure in the work-place and through the diet, and suspicion of toxicity based on existing data as well as structural similarity to known rodent reproductive toxicants and carcinogens [10].

Advanced oxidation processes (AOPs) are at present considered to have great potential in degrading chlorinated organic compounds. AOPs make use of different reacting systems, including photochemical degradation processes (UV/O_3, UV/H_2O_2), photocatalysis (TiO_2/UV, photo-Fenton reagent), and chemical oxidation processes (O_3, O_3/H_2O_2, H_2O_2/Fe^{2+}). The light driven AOPs involve the production of hydroxyl radicals, which react almost non-selectively with the organic pollutants at very high rates. Chemical treatment of wastewaters by AOPs can result in the complete mineralization of the pollutants to carbon dioxide, water, inorganic compounds or, at least, in their transformation to harmless end products.

Low-pressure mercury vapor lamps with a 254 nm peak emission are the most common UV source used in H_2O_2/UV systems. UV radiation is absorbed by water and affects the water photolysis leading to the production of hydroxyl radicals and also, photolysis of H_2O_2 yields hydroxyl radicals by a direct process with a yield of two radicals formed per photon absorbed by 254 nm. In this case, a high concentration of H_2O_2 is needed to generate sufficient hydroxyl radicals [11].

AOPs also make use of catalysts such as ZnO [12,13], CdS and SnO_2 [14], cobalt [15]. Most of the research is done on semiconductor photocatalysis for water purification using TiO_2 powder dispersions. The use of such slurries obviously requires a subsequent separation step involving either filtration, centrifugation or coagulation/

* Corresponding author. Tel.: +30 210 7723224; fax: +30 210 7723155.
E-mail address: kphilip@chemeng.ntua.gr (C.J. Philippopoulos).

0926-3373/$ – see front matter © 2009 Elsevier B.V. All rights reserved.
doi:10.1016/j.apcatb.2009.02.018

flocculation which instantly compromises the system's economical viability. However, slurry reactor photocatalytic systems are usually very efficient in terms of photons (relative to thin film reactors) and easy to make and maintain. TiO_2 is currently considered as the most promising photocatalyst because of its reasonable photocatalytic activity, relatively low cost, and high stability toward photocorrosion [12,16–18]. However, recent research questions the absence of toxicity of TiO_2 indicating that nanosize TiO_2 could pose a risk to biological targets that are sensitive to oxidative stress damage [19]. The primary mechanism of photodegradation is the generation of hydroxyl radicals obtained by the reaction of holes with surface hydroxyls or water and their attack to organic compounds. Hydroxyl radicals are very reactive species; they react rapidly and non-selectively with organic compounds and are the common oxidizing agent [11].

However, the application of TiO_2 for photocatalytic oxidation of organic molecules is limited by both high charge carrier recombination rates and, usually, the need for ultraviolet excitation [20]. Also, some reports indicated that doping with a group of transitional metal ions, depositing some noble metals such as Au and Pt, and coupling metallic oxides into TiO_2 lattice are effective strategies for reducing the recombination of electron–hole pairs significantly and also extending the light response of TiO_2 in the visible region. Furthermore, lanthanide ions can form complexes with various Lewis bases including organic acids, amines, aldehydes, alcohols, and thiols by interaction of the functional groups with their f orbital. Thus, doping lanthanide ions into a TiO_2 matrix can concentrate organic pollutants on the semiconductor surface and therefore improve the photoactivity as well as extend the photoresponse in the visible region [21]. The doping of TiO_2 by Fe(III) which modifies its structure and/or its morphology and accordingly may also modify the photocatalytic activity is also reported in the literature [22].

Regarding the use of catalysts in AOPs, certain areas that require further investigation include: the understanding of the degradation mechanisms, reaction and intermediates involved; the optimization in the catalyst structure in order to reduce the amount of reagent chemical required, and hence the associated cost [11].

In this study, were prepared catalysts using as substrate TiO_2 P25 with three different metals (Pt, Ce, Fe) and XRD characterization was performed. Primarily, the effect of these catalysts was studied on hydrogen peroxide degradation in a batch reactor under UV irradiation. Also, the feasibility of treating 1,3-dichloro-2-propanol in a batch reactor under UV irradiation with the prepared catalysts was examined and a kinetic study was performed in order to assess their efficiency and calculate the rate constants. Finally, a degradation pathway is proposed for the 1,3-DCP degradation based on the intermediates identified.

2. Materials and methods

2.1. Photoreactor

The photochemical and photocatalytical oxidation of 1,3-DCP was investigated with a photoreactor (Heraeus Noblelight UV-RS-3) that consists of a low-pressure Hg lamp of 15 W, which produces ultraviolet light of 253.4 nm, immersed in the center of a glass cylindrical vessel 1000 mL volume. 1,3-DCP was dissolved in water (initial concentration 0.024 M). Simultaneously when adding the hydrogen peroxide and/or the catalyst, the light was turned on. During the reaction, the solution was maintained in suspension by magnetic stirring. The solution pH was measured during the experiment for observing the progress of the reaction by a WTW-pH90 pH-meter. No significant differences were observed in pH evolution among the different experimental conditions investigated. For all the catalysts employed in this study the initial pH value of the solution was approximately 5.20 and after the lamp was turned on, the pH value dropped in the range of 3. The pH in the reactor solution was not controlled in the experiments performed, since the pH value of 3 is also used in the literature for the oxidation of chlorinated organic contaminants in the presence of UV radiation [18].

2.2. Chemicals

All reagents were used as received without any further purification. Freshly prepared 1,3-DCP solutions were used. The initial concentration of each 1,3-DCP solution was 0.024 M. H_2O_2 solution, 30% (w/w) (Merck), was used as an additional source of hydroxyl radicals. Only deionized water was used.

2.3. Catalyst preparation

Catalyst preparation was based on titania powder (Degussa P25). Three powders were prepared based on P25 and enriched with 1%Pt as hexachloroplatinic (IV) acid (Cl_6H_2Pt) solution about 10% (Merck), 10% Ce as cerium nitrate (REacton) $CeN_3O_9{\cdot}6H_2O$, 10%Fe as $Fe(NO_3)_2$ non-hydrate (Sigma–Aldrich). The mixtures were prepared in methanol and, as the crystal structures of the TiO_2 depend on the sintering, they were sintered for 3 h at 450 °C. A preliminary set of experiments was performed in order to estimate the optimum catalyst loading for our photoreactor, and these experiments (not presented here) indicated that 65 mg/L of catalyst load led to the best results. Therefore, 65 mg/L of catalyst were added in the reactor solution as a suspension.

2.4. Photocatalyst characterization

The crystalline structure of the prepared P25 TiO_2-based catalysts were analyzed by using a Siemens D5000 diffractometer with Cu Kα radiation operated at 40 kV and 30 mA at a scan rate of 1.2°/min. The crystallite size of the samples, d_{XRD}, can be estimated from XRD patterns by the Scherrer equation:

$$d_{XRD} = \frac{0.9\lambda}{\mathrm{FWHM}\cos\theta}$$

where λ is the X-ray wavelength (1.5406 Å), FWHM (in radians) is the full width at half maximum of the characteristic peak (1 0 1) of TiO_2 and θ is the diffraction angle for the (1 0 1) plane.

2.5. Sample preparation for analysis

In order to determine quantitatively the concentration of 1,3-dichloro-2-propanol, 1 μL taken from the reactor was analyzed in the GC–MS. All aliquots were filtered through a syringe filter with pore size 0.45 μm. In order to identify the oxidation intermediates a 5 mL liquid sample was withdrawn from the reactor and the organic compounds contained in the sample were extracted and condensed to 1 mL of chloroform after vigorous stirring. The sample was allowed 15 min to stabilize and 1 μL was taken from the organic phase and analyzed in the GC–MS.

2.6. Analytical instruments

Gas chromatography–mass spectroscopy analysis (Hewlett Packard GC 6890–MS 5973, column HP1-MS) was employed for determining 1,3-DCP concentration and for detection of oxidation intermediates. The chromatograms obtained were analyzed via a personal computer and the appropriate software (HP Chemstation). The program used for sample analysis was the following: the oven was set at 50 °C for 1.50 min, then the temperature increased

at a rate of 50 °C/min up to 150 °C and remained stable for 1 min, then the temperature increased at a rate of 10 °C/min up to 200 °C, and with 20 °C/min up to 240 °C, total duration 11.50 min. The concentrations of total carbon (TC), inorganic carbon (IC), and total organic carbon (TOC) were measured with a total organic carbon analyzer (TOC-V 108 CSH, Shimadzu). A DX600 Ion Chromatographer Dionex (column: IonPac AS9-HC 4 mm) was used for the qualitative and quantitative determination of chloride ion, chloroacetic, formic and acetic acids. The chromatograms obtained were analyzed by means of a personal computer and the appropriate software (Peaknet 6, Version 6.4). The H_2O_2 concentration was measured using the standard titanate (IV) method in a UV–Vis spectrophotometer (PerkinElmer).

3. Results and discussion

3.1. XRD spectra of samples

Fig. 1 presents the XRD patterns of the P25 TiO_2-based catalysts prepared in this work in comparison to the spectrum of P25 TiO_2 as well as to the spectrum of P25 after following the same procedure that the modified catalysts underwent that is designated as TiO_2P25b.

Also, in Table 1 are listed the crystallite sizes for each catalyst as were calculated by the Scherrer equation. Apparently, the annealing temperature had an effect on the grain size of TiO_2 and more specifically annealing at 450 °C the peak intensities of anatase steadily become stronger and the width of the diffraction peak of anatase slightly becomes narrower, indicating the formation of greater TiO_2 crystallites and the enhancement of crystallization of TiO_2 [23].

A comparison between the XRD patterns of the two TiO_2P25 samples, indicated that the annealing process caused a slight increase in the crystallite size. The XRD pattern of Pt/TiO_2 sample showed a peak at 39.7° indicating the incorporation of platinum in the TiO_2 lattice. The XRD pattern of Ce/TiO_2 sample showed a peak at 28.7° characteristic of the presence of CeO_2 in the lattice. The XRD pattern of Fe/TiO_2 sample showed a peak at 33.4° that can be attributed to the formation of Fe_2O_3 or $FeTiO_3$ indicating the incorporation of ferrum in the TiO_2 lattice. Since no peak broadening was observed, no defects arose in the crystal.

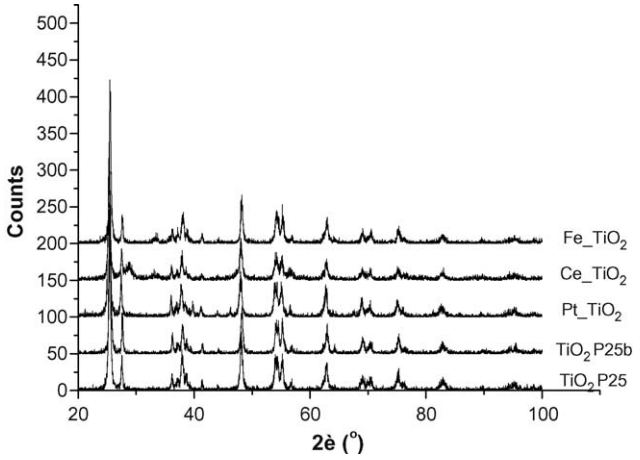

Fig. 1. XRD patterns of the prepared TiO_2 catalysts.

Table 1
Calculated crystallite sizes of the prepared catalysts.

Sample	Crystallite size (nm)
TiO_2 P25	20.89
TiO_2 P25b	22.89
Pt/TiO_2	19.81
Ce/TiO_2	20.30
Fe/TiO_2	21.51
Rh/TiO_2	18.36

3.2. Hydrogen peroxide degradation

Hydrogen peroxide is widely used either alone or in combination with other treatment processes in environmental applications. H_2O_2 in water is a rather mild and ineffective oxidant without light or metal ion catalysis [24]. It can also serve as a reducing agent as well as an oxidizing agent [25]. Decomposition of H_2O_2 in water depends on temperature, pH, and presence of impurities (e.g. metal ions, metal oxyhydroxides). The photolysis of H_2O_2 to yield reactive and nonselective hydroxyl radicals is an important indirect method of contaminant destruction [26]. Enhanced degradation of organic pollutants by UV/H_2O_2 system is well known. The addition of photocatalysts and thermal catalysts to H_2O_2 has also been shown to promote effective contaminant destruction [27,28]. Therefore, prior to performing the photochemical/photocatalytical experiments a series of experiments was performed in the reactor in order to investigate the degradation of hydrogen peroxide for two different initial concentrations and under different oxidative conditions. Namely, for H_2O_2 concentrations 0.081 M and 0.163 M, under UV irradiation and in the presence of 65 mg/L TiO_2 P25, 65 mg/L Pt/TiO_2, 65 mg/L Ce/TiO_2, 65 mg/L Fe/TiO_2.

The conversion of hydrogen peroxide for initial concentration 0.081 M is presented in Fig. 2(a). As it can be seen, 100% H_2O_2 degradation was accomplished for all experimental conditions except from the use of UV radiation alone. The conversion of hydrogen peroxide for initial concentration 0.163 M is presented in Fig. 2(b).

For the kinetic study of H_2O_2 degradation four different models were evaluated: (a) zero-order, (b) first-order, (c) *n*-order, (d) Langmuir–Hinshelwood. Regarding the models evaluated, it should be noted that recent studies by Emeline et al. [29,30] point out the existence of misconceptions in the assumptions made concerning the implementation of Langmuir–Hinshelwood kinetics to photocatalytic reactions. These studies provide a possible explanation to the fact that the Langmuir–Hinshelwood model provided a poor fit to our results. Among the models evaluated, the best fit to the experimental data was provided by the zero-order kinetic expression. The apparent rate constants for each set of conditions as well as the sum of the squares of experimental and calculated concentrations are shown in Table 2. The value of the apparent rate constants remained roughly unaffected by the addition of catalysts as well as by the change in the initial hydrogen peroxide concentration, indicating that H_2O_2 degradation depends only upon the radiation emitted by the lamp.

In the literature controversial results are found regarding the kinetic expression for hydrogen peroxide homogeneous degradation. More specifically, Carlton et al. [31] employed the same Heraeus Noblelight photochemical batch reactor as the one used in this study for the photooxidation of oxalic acid. The calculated first-order kinetic constant was 10^{-4} s^{-1} for the production of two $OH^{\bullet}$ per H_2O_2 molecule for initial H_2O_2 concentrations 8–10 mM. In our study for initial H_2O_2 concentrations 81 and 163 mM the zero-order kinetic rate constants were in the range of 0.1×10^{-4} mol L^{-1} s^{-1}. Also, Ilisz et al. [32] have calculated the zero-order rate constant $((1.9 \pm 0.2) \times 10^{-8}$ M s^{-1} for $[H_2O_2]_0 = 0.01$ M), while they also concluded that that the observed H_2O_2 photodecomposition is determined by the UV photons

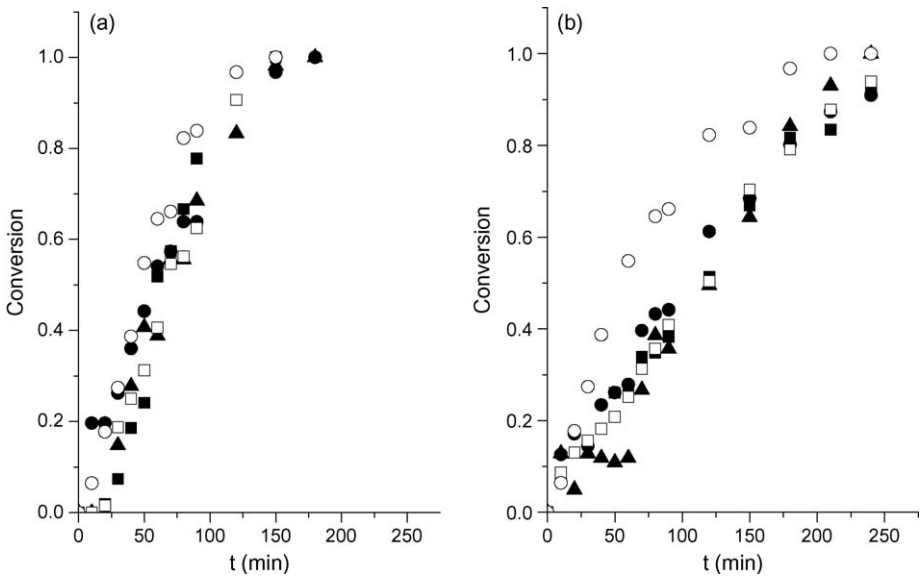

Fig. 2. H_2O_2 conversion for initial hydrogen peroxide concentration 0.081 M (a) and 0.163 M (b) under UV radiation (■), P25/UV (●), Pt/TiO_2/UV (▲), Ce/TiO_2/UV (□), Fe/TiO_2/UV (○).

impinging on the suspension. On the other hand, Adán et al. [33] used a first-order kinetic expression to describe their results for a 500 W high-pressure Hg lamp at a wavelength of 365 nm and the value estimated for the first order rate constant was 5.6×10^{-7} M s^{-1}. The H_2O_2 apparent rate constants calculated in this study are higher than the ones found in the literature.

3.3. 1,3-DCP degradation experiments

Experiments with two different initial hydrogen peroxide concentrations were carried out for studying the photo-oxidation of 1,3-DCP in aqueous solutions, whereas the initial 1,3-DCP concentration was held constant at 0.024 M. All experiments were conducted under UV irradiation. Reactor samples were collected at specific time intervals.

3.3.1. Comparison between UV/H_2O_2 and TiO_2 P25/UV/H_2O_2 process

Fig. 3 presents the results of the photo-catalytic oxidation under UV irradiation and with the use of 65 mg/L TiO_2 in terms of TOC removal $((C_o - C)/C_o)$ 1,3-DCP conversion and chloride ion production. Increasing the amount of H_2O_2 from 0.081 M to 0.163 M increased TOC removal and more specifically, under UV irradiation alone TOC removal increased from 20% to 35%, while for TiO_2/UV the respective increase was from 23% to 35%. Also, for initial H_2O_2 concentration 0.081 the addition of 65 mg/L TiO_2 showed a tendency to increase TOC removal and to decrease chloride ion production. The decrease in the dechlorination degree of the reactor solution indicated that the presence of Cl^- affects the behavior of TiO_2. According to Parsons [11], chloride is responsible for hydroxyl radical scavenging. Particularly in iron catalyzed decomposition of hydrogen peroxide the kinetic study showed that the rates of decomposition of H_2O_2 decreased in the presence of chloride [34]. An inhibitory effect of chloride ion has also been observed for the oxidation by Fe(II)/H_2O_2 or by Fe(III)/H_2O_2 of 4-chlorophenol [35,36], 2,4-dichlorophenol in Na_2SO_4 solution [37], dichlorvos [38], dyes [39–41], acetic acid, atrazine and 4-nitrophenol [42], phenol [43] and aniline [44].

Table 2
Hydrogen peroxide degradation apparent rate constants under different experimental conditions.

	k (mol $L^{-1}s^{-1}$) × 10^{-4}	$\Sigma(C_{exp} - C_{calc})^2 \times 10^{-4}$
$[H_2O_2]_0$ = 0.081 M		
UV/H_2O_2	0.100	6.120
TiO_2	0.081	6.110
Pt-TiO_2	0.091	2.831
Ce-TiO_2	0.109	2.831
Fe-TiO_2	0.127	2.698
$[H_2O_2]_0$ = 0.163 M		
UV/H_2O_2	0.103	6.12
TiO_2	0.096	11.34
Pt-TiO_2	0.084	4.129
Ce-TiO_2	0.103	8.101
Fe-TiO_2	0.126	2.225

3.3.2. Photocatalytical oxidation with catalysts based on TiO_2

Fig. 4 shows the results for initial H_2O_2 concentration 0 M, 0.081 M and 0.163 M for the three different modified catalyst suspensions tested. The best results for the photocatalytic oxidation in the absence of H_2O_2 arose in the case of Fe/TiO_2, where 1,3-DCP conversion reached 36%. Also, for Fe/TiO_2 increasing the amount of H_2O_2 increased remarkably TOC removal, 1,3-DCP conversion and chloride ion production. For $[H_2O_2]_0$ = 0.081 M and for Fe/TiO_2, the lowest TOC removal (10%), DCP conversion (40%) and chloride ion production (40%) among the catalysts examined were obtained. The behavior of Fe/TiO_2 catalyst in our system was complicated. According to Araña et al. [45], where the photocatalytic degradation of maleic acid by using Fe-doped (0.15, 0.5, 2 and 5%, w/w in Fe) TiO_2 catalysts was studied, catalysts with the lowest Fe content (0.15 and 0.5%) showed a considerably better photocatalytic behavior than non-doped TiO_2, whereas with the use of catalysts with higher Fe contents smaller conversions arose. Since in our experiments a catalyst with a high Fe content (10%) was prepared, our findings for 1,3-DCP degradation using a Fe/TiO_2 catalyst are in agreement with the cited study.

For Pt/TiO_2 and Ce/TiO_2 increasing the initial H_2O_2 concentration did not affect the results in terms of TOC removal and 1,3-DCP conversion. On the other hand chloride ion production decreased when $[H_2O_2]_0$ increased from 0.081 to 0.163 M. Also, by the use of the Pt/TiO_2 suspension the best TOC removal was achieved (40%). For $[H_2O_2]_0$ = 0.163 M, 1,3-DCP conversion was in the order of 93% for all catalysts examined.

Comparing the results for the catalysts prepared to the use of TiO_2/P25, we observe that modifying TiO_2 with platinum and

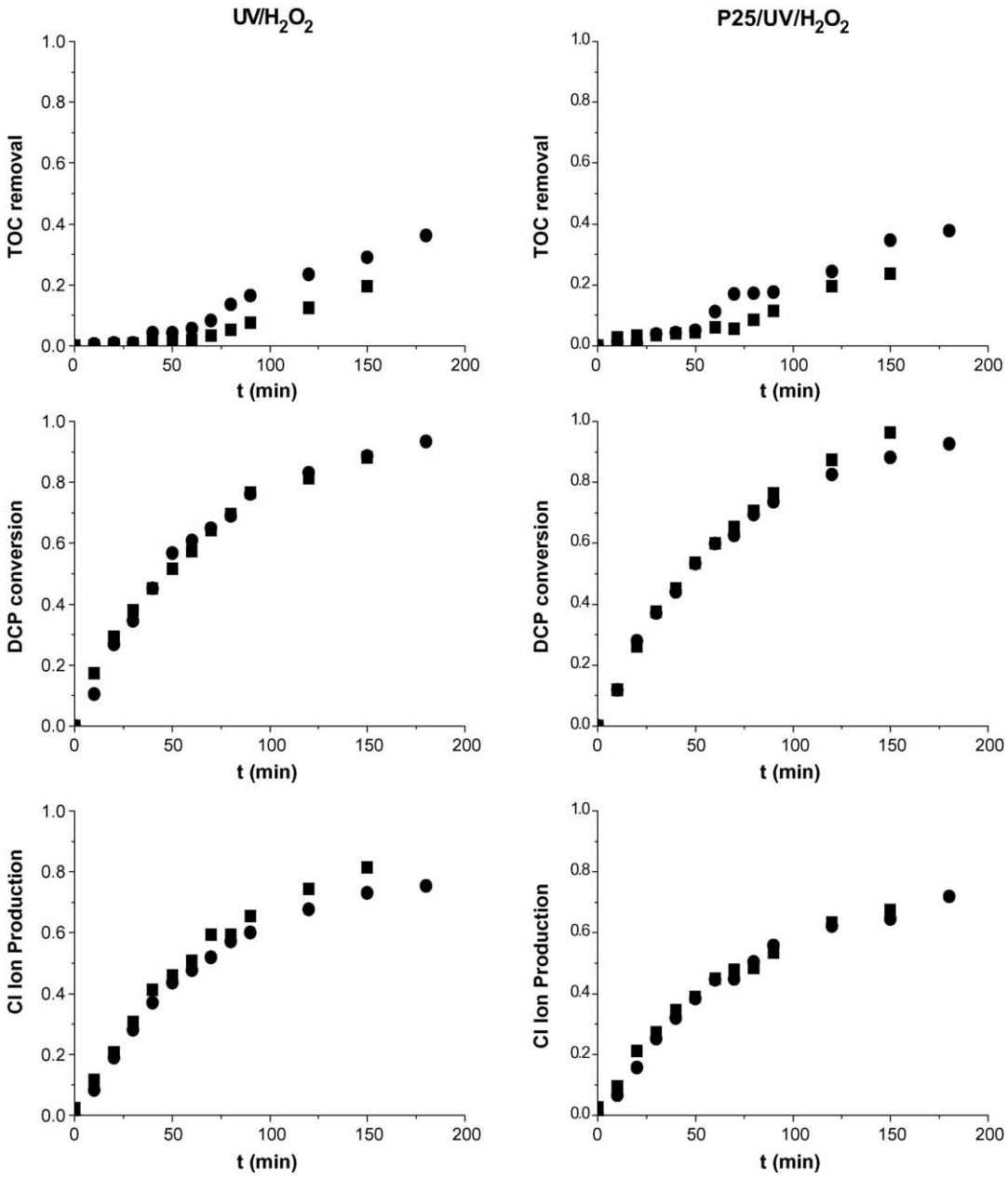

Fig. 3. TOC removal, 1,3-DCP conversion and chloride ion production for initial hydrogen peroxide concentration 0.081 M (■) and 0.163 M (●) under UV irradiation and with 65 mg/L TiO_2/UV.

cerium improved the removal of total organic carbon, particularly for the lower initial hydrogen peroxide concentration. Also, comparing the photochemical and the photocatalytical process for catalysts TiO_2/P25, Pt/TiO_2, Ce/TiO_2, it can be seen that TOC removal and 1,3-DCP conversion increased with the addition of catalyst.

Fig. 5 shows the behavior of organic acids (acetic, formic and chloroacetic acid) arising as intermediates of 1,3-DCP oxidation under different experimental conditions. In the case of complete lack of oxidative agent, $[H_2O_2]_0 = 0$ M, for all catalysts tested, the organic acids production remained at low levels throughout the experiments. Acetic and formic acids were gradually produced as the reaction proceeded, while the concentration of chloroacetic acid remained stable. For $[H_2O_2]_0 = 0.081$ M, the concentration of organic acids for Fe/TiO_2 was significantly lower in comparison to the other experiments. Except from Fe/TiO_2 for $[H_2O_2]_0 = 0.081$ M, acetic acid was produced and after 120 min reaction time it was slowly consumed, while chloroacetic acid was notably consumed in the presence of TiO_2/P25/UV. For $[H_2O_2]_0 = 0.163$ M the concentration of organic acids rose and then decreased indicating the fact that they were further oxidized. A general remark drawn by the organic acids behavior is that increasing the initial hydrogen peroxide concentration increased the amount of organic acids produced in the reactor.

3.4. Intermediates—pathway

The oxidation intermediates identified by GC–MS analysis as well as a proposed degradation pathway are shown in Fig. 6. Since, chloroacetic, acetic and formic acids were also quantitatively determined, it was established that the route following the production of chloroacetic chloride from 1-chloro-2-propanone prevailed against the production of chloromethyl-2-chlorobutanoate and chloromethyl-3-chlorobutanoate.

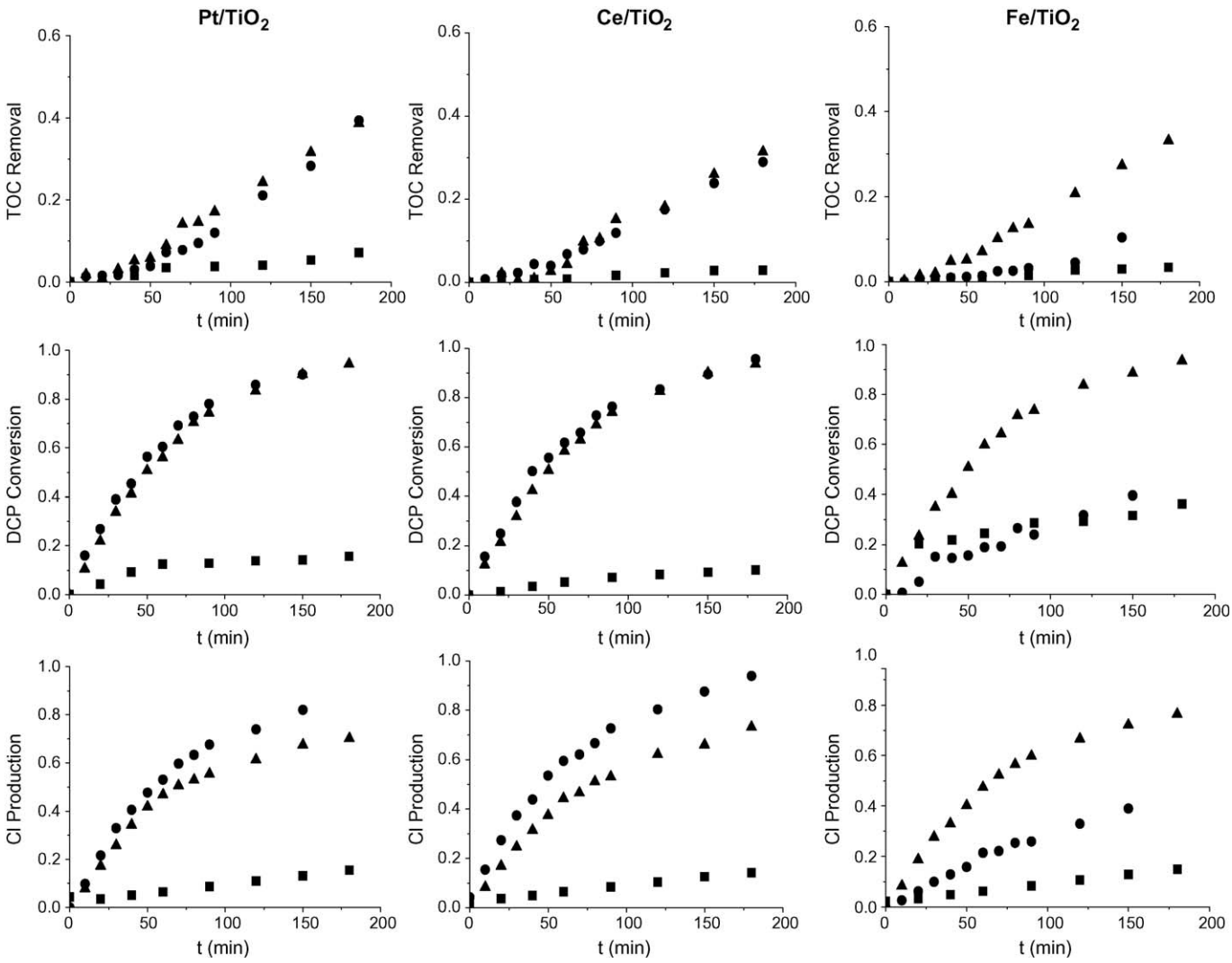

Fig. 4. TOC removal, 1,3-DCP conversion and chloride ion production in the absence of H_2O_2 (■) and for initial hydrogen peroxide concentrations 0.081 M (●) and 0.163 M (▲) for the three different catalysts.

It should be noted that in absence of H_2O_2 and in the presence of catalysts some initial oxidation products were being produced without being consumed. More specifically, chloromethyl-2-chlorobutanoate and chloromethyl-3-chlorobutanoate accumulated in the reactor solution and the reaction did not proceed any further in this direction. Also, even though chloroacetic acid was produced in the first 20 min, formic acid arose after 60 min reaction time and acetic acid after 120 min.

For $[H_2O_2]_0$ = 0.163 M during photochemical and photocatalytical oxidation, chloromethyl-2-chloropropanoate and chloromethyl-3-chloropropanoate were not detected. However, since 3-chloropropanoyl chloride, 2-chloropropanoyl chloride and chloropropionic acid were produced, we assume that the "propanoates" were produced and consumed very fast, rendering their detection not possible. Anipsitakis et al. [46] observed that chloride ions reacted with sulfate radicals to form chlorine radicals that reacted with the organic material to give rise to the chlorinated derivatives detected from the transformation of 2,4-dichlorophenol and phenol. In this study, since chloride ion production increased in the presence of H_2O_2 under all experimental conditions investigated in this work and rose above 80%, the presence of chloride ions in the reactor solution indicated that they did not affect the formation of the oxidation products.

The microorganisms that have the ability to biodegrade 1,3-dichloro-2-propanol are bacteria such as *Corynobacterium sp.* and *Arthrobacter sp.* A proposed microbial transformation pathway [6,7] suggests two possible routes: 1,3-dichloro-2-propanol, (RS)-3-chloro-1,2-epoxypropane, (RS)-3-chloro-1,2-propanediol, (RS)-3-hydroxy-1,2-epoxypropane, glycerol. 1,3-Dichloro-2-propanol, (R)-3-chloro-1,2-epoxypropane, (R)-3-chloro-1,2-propanediol, (R)-3-hydroxy-1,2-epoxypropane, glycerol. On the other hand, pure pseudomonas cultures degraded 1,3-DCP to 1-chloro-2,3-propylene glycol, glycidol, epichlorohydrin and glycerol. The biodegradation of DCP by bacteria may therefore lead unfortunately to the production of epichlorohydrin, which more toxic than DCP.

Generally, chlorinated compounds exhibit resistance to biodegradation, and chemical oxidation is usually employed to treat solutions of these compounds prior to biological process [47]. The knowledge of the intermediates produced during the photochemical/photocatalytical oxidation of 1,3-dichloro-2-propanol is of great importance, if the process is to be combined with a biological unit. Moreover, 1,3-DCP is a hydrolysis product and metabolite of the carcinogen epichlorohydrin, and epichlorohydrin may be formed from 1,3-DCP by the action of bacterial enzymes. Because epichlorohydrin slowly hydrolyzes in water at neutral and lower

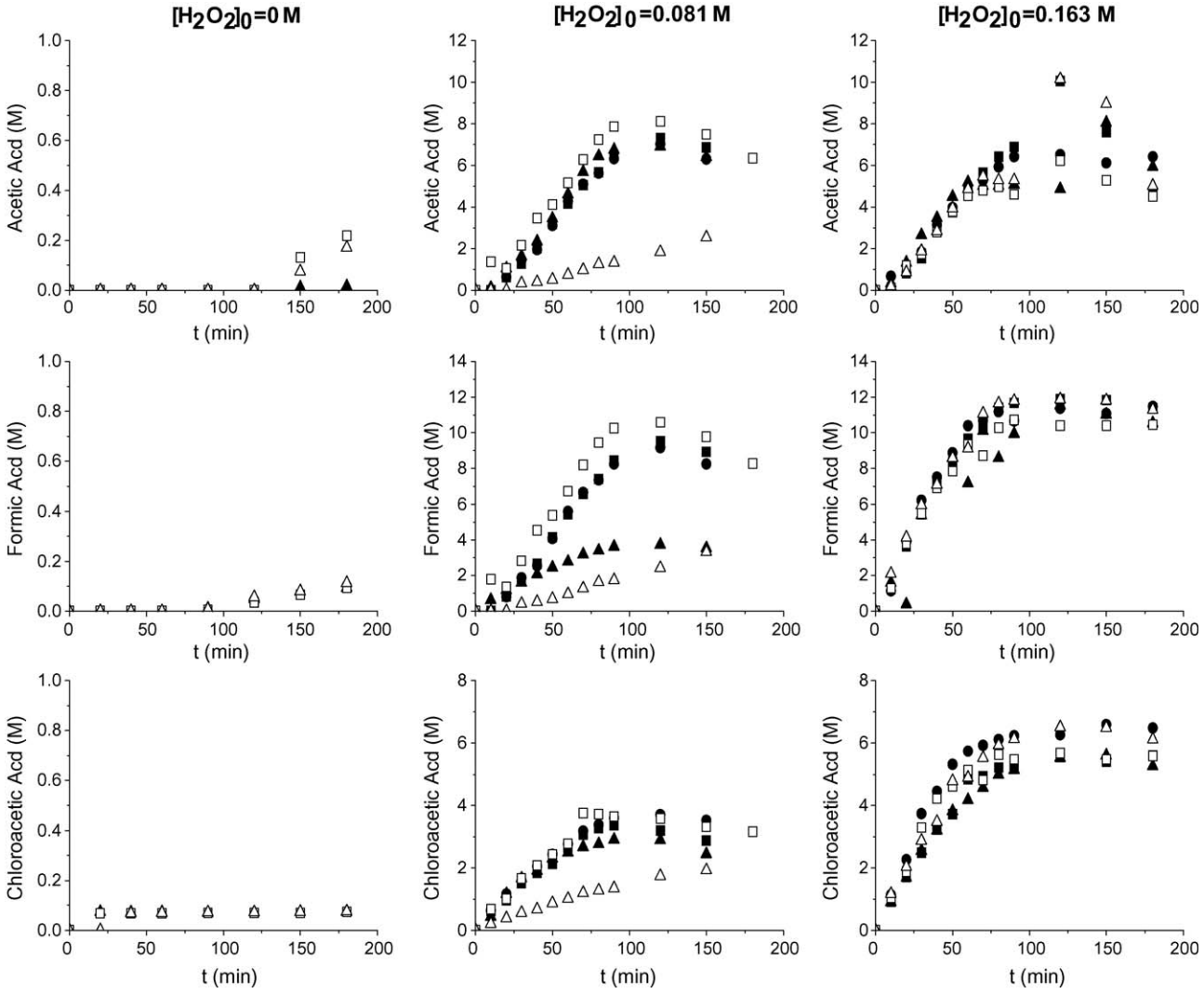

Fig. 5. Acetic, formic and chloroacetic acid production for three different initial hydrogen peroxide concentrations under UV irradiation (■), in the presence of 65 mg/L catalyst TiO_2/P25/UV (●), Pt/TiO_2/UV (▲), Ce/TiO_2/UV (□), FeTiO_2/UV (△).

pH, epichlorohydrin releases to air and water are sources of environmental chloropropanols [10]. The oxidation processes investigated in this study have the ability to completely degrade DCP in aqueous solutions, whereas simultaneously the reacted chlorine was converted quantitatively to chloride ion, indicating that the chlorinated structures were effectively destroyed. Therefore, the elimination of the initial compound in combination with the removal of chloride taking place makes this process attractive to being employed as a primary step prior to biodegradation processes.

3.5. Kinetic study

Based on the data acquired by the experiments performed in this study a kinetic analysis of the UV/H_2O_2 process, using TiO_2, Ce/TiO_2, Fe/TiO_2, Pt/TiO_2 catalysts, for the oxidation of 1,3-DCP was conducted. The reaction mechanism was developed using the concentrations of 1,3-DCP, the production of the organic acids arising as intermediates and the TOC measurements. The experimental results led to the following observations: (a) 1,3-DCP degradation followed pseudo-first-order kinetics, (b) the organic acids concentrations initially rose and then decreased or remained approximately stable and (c) TOC measurements indicated the mineralization taking place during the reaction. According to these observations several series of parallel reactions were assumed and the one indicating the best fitting on the experimental data is presented here. The reaction model involves the following steps:

$$C_3H_6Cl_2O + H_2O_2 \xrightarrow{k_1} I \quad (1)$$

$$I + H_2O_2 \xrightarrow{k_2} CO_2 + H_2O + HCl \quad (2)$$

$$I + H_2O_2 \xrightarrow{k_3} CH_3COOH + HCl + H_2O \quad (3)$$

$$I + H_2O_2 \xrightarrow{k_4} HCOOH + CO_2 + HCl + H_2O \quad (4)$$

$$I + H_2O_2 \xrightarrow{k_5} ClCH_2COOH + HCl + H_2O \quad (5)$$

$$ClCH_2COOH + 2H_2O_2 \xrightarrow{k_6} CO_2 + HCOOH + HCl + 2H_2O \quad (6)$$

$$CH_3COOH + 3H_2O_2 \xrightarrow{k_7} CO_2 + HCOOH + 4H_2O \quad (7)$$

where, k_i are the reaction kinetic constants (s^{-1}) and I represents the total chlorinated organic intermediates except from chloroacetic acid, that was separately determined quantitatively. The implementation of several reaction schemes prior to establishing the one with the best fit presented thoroughly in this work led to

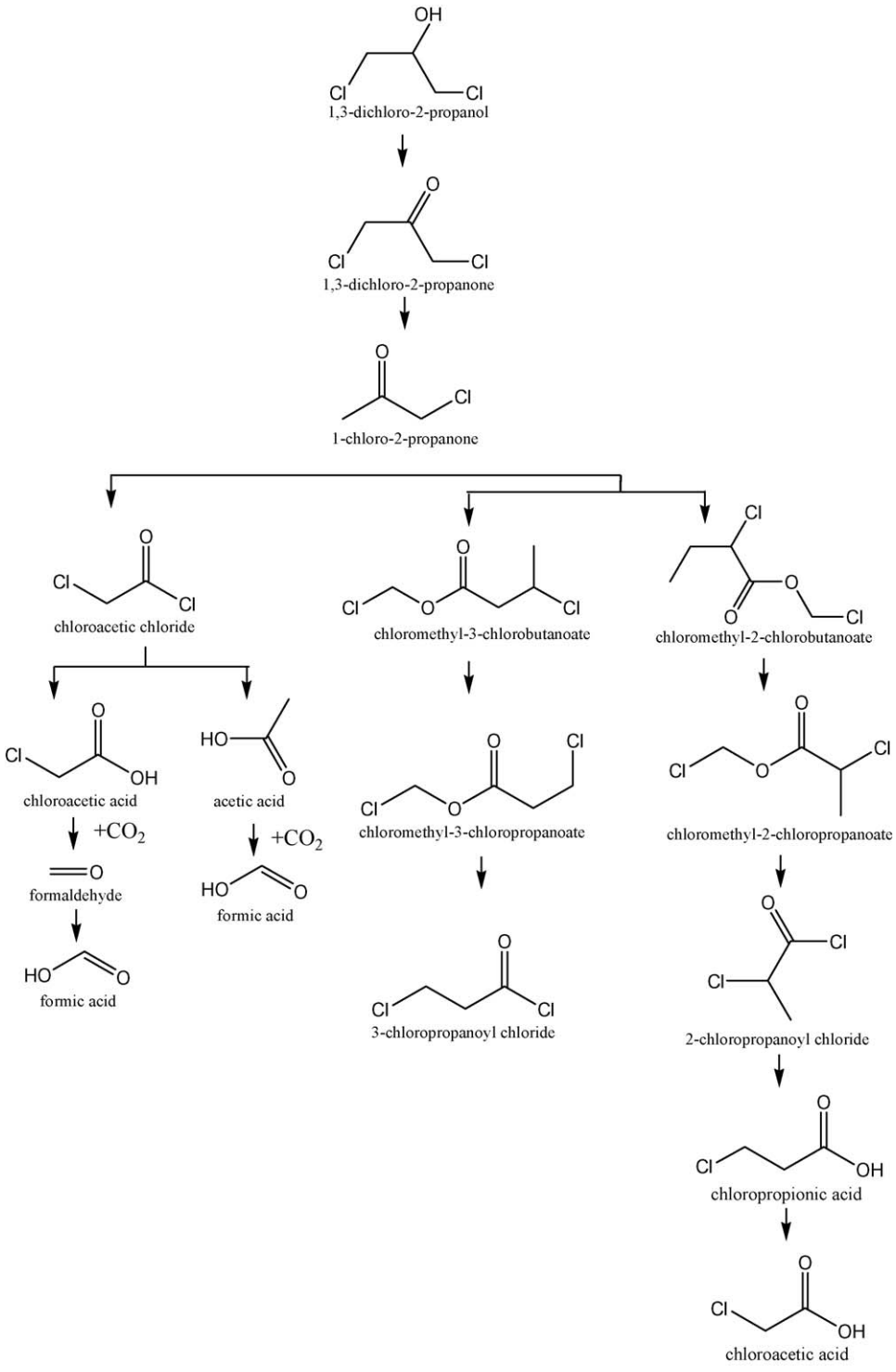

Fig. 6. A proposed pathway for 1,3-DCP oxidation.

the following observations: (a) reaction schemes leading to the direct CO_2 production from 1,3-DCP did not fit the experimental data and (b) formic acid was resistant to oxidation and did not degrade to CO_2. The model proposed for 1,3-DCP degradation comprises of reactions (1)–(7). Also, the best fit to the experimental results arose by the implementation of first-order kinetics. This can be explained if the inhibition due to adsorption is assumed negligible, that is if the chemical reaction is the controlling step of the process, which was also verified by the results regarding DCP conversion and TOC removal as shown in Fig. 4 in the absence of H_2O_2.

A system of differential equations has been postulated based on mass balance calculations for the particular model. The unknown k_i parameters have been estimated by fitting the model to the experimental data (using MathCAD version 12 by Mathsoft) by means of a nonlinear regression analysis (a fixed-step Runge–Kutta method). The objective function, the sum of squares of the differences between the experimental and the calculated values of

Table 3
Estimated kinetic parameters for $[H_2O_2]_0 = 0.081$ M and $[H_2O_2]_0 = 0.163$ M.

	$k_1 \times 10^{-4}$	$k_2 \times 10^{-4}$	$k_3 \times 10^{-4}$	$k_4 \times 10^{-4}$	$k_5 \times 10^{-4}$	$k_6 \times 10^{-4}$	$k_7 \times 10^{-4}$
$[H_2O_2]_0 = 0.081$ M							
UV/H_2O_2	2.696	0.054	0.978	0.066	0.719	2.328	0.629
TiO_2	2.727	0.715	0.725	0.481	0.355	3.305	0.311
Pt/TiO_2	2.685	0.091	1.471	0.293	0.635	1.215	1.259
Ce/TiO_2	2.579	0.834	1.126	0.613	0.769	0.881	0.052
Fe/TiO_2	0.628	0.202	0.378	0.368	0.343	0.005	0.008
$[H_2O_2]_0 = 0.163$ M							
UV/H_2O_2	2.598	1.475	1.931	0.968	1.632	0.410	0.420
TiO_2	2.413	3.327	2.426	1.984	3.254	0.391	0.014
Pt/TiO_2	2.112	4.020	1.966	1.942	1.959	1.011	0.001
Ce/TiO_2	2.272	1.283	1.256	0.899	1.546	0.446	0.158
Fe/TiO_2	2.401	1.951	2.253	1.519	2.392	0.404	0.077

k_i: s^{-1}.

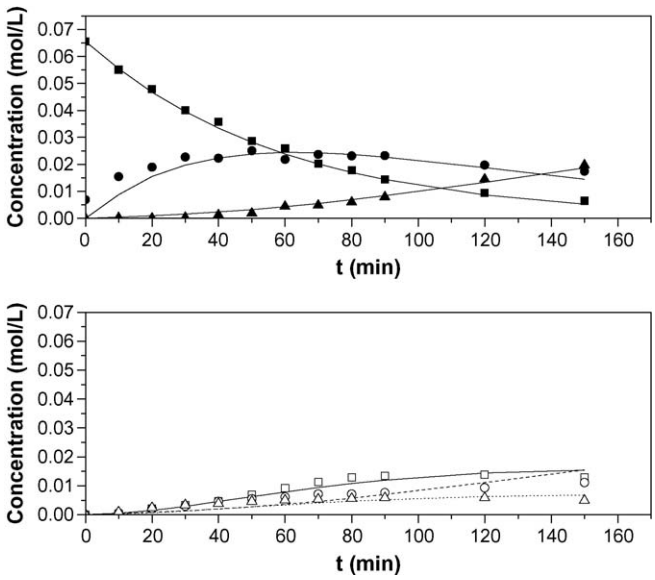

Fig. 7. A comparison of calculated concentrations with experimental data under H_2O_2/UV process by the use of Pt/TiO_2 and $[H_2O_2]_0 = 0.081$ M, lines: estimated concentration, 1,3-DCP_{exp} (■), I_{exp} (●),$CO_{2\ exp}$ (▲), acetic $acid_{exp}$ (□), formic $acid_{exp}$ (○),chloroacetic $acid_{exp}$ (△).

concentrations, was minimized by the nonlinear Levenberg–Marquardt algorithm in order to determine the reaction rate coefficients. Finally the solution obtained was tested and compared to the experimental results. Fig. 7 presents an example of the comparison between calculated and experimental data. The estimated k_i parameters are reported in Table 3.

In the case of complete lack of oxidative agent, $[H_2O_2]_0 = 0$, and with the use of the catalysts, as it can be seen in Fig. 5 chloroacetic acid and acetic acid were not oxidized any further and their concentrations rose with reaction time as they accumulated in the reactor. With the addition of hydrogen peroxide into the reactor solution the experimental data show that the oxidation proceeds further to the formation of formic acid and carbon dioxide from chloroacetic and acetic acid, and the values of the calculated rate constants are also presented in Table 3.

By the catalyst's addition a significant increase is noted in the values k_2 in comparison to the photochemical process for both hydrogen peroxide concentrations, corresponding to the direct mineralization of the chlorinated intermediate I, and explaining the reason why introducing the catalysts in the reactor increased the total organic carbon removal.

From Table 3, it is obvious that for each catalyst increasing the initial hydrogen peroxide concentration from $[H_2O_2]_0 = 0.081$ M to $[H_2O_2]_0 = 0.163$ M is followed by an increase in rate constants k_1–k_5. This means that reactions (1)–(5) in the proposed reaction scheme took place at a higher rate, whereas the oxidation of chloroacetic and acetic acid to formic acid and CO_2 was limited (k_6, k_7).

In general, the addition of the catalyst did not affect the oxidation rates of 1,3-DCP to the chlorinated intermediate I (k_1) for neither of the initial hydrogen peroxide concentrations investigated in this work, except from the case of Fe/TiO_2 for $[H_2O_2]_0 = 0.081$ M, where k_1 is remarkably lower. This is in total agreement with the results for 1,3-DCP conversion shown in Fig. 4, where the maximum 1,3-DCP degradation after 150 min reaction time was 40% in contrast to the other catalysts that reached 100% conversion.

For $[H_2O_2]_0 = 0.081$ M and for catalyst suspensions of TiO_2/P25 and Ce/TiO_2 while the highest k_2 values (mineralization of I) are noted, TOC removal was 23% and 30%, respectively, whereas the highest TOC removal was 40% for Pt/TiO_2. This can be explained by the fact that although k_2 has a low value for platinum, the carbon dioxide production is attributed to high values for both k_6 and k_7 (production of formic acid and carbon dioxide by chloroacetic acid and acetic acid degradation).

The kinetic investigation for $[H_2O_2]_0 = 0.163$ M showed that with the use of the Pt/TiO_2 catalyst arose the highest k_2 value, corresponding to the degradation of the chlorinated intermediate I to CO_2. Also, the addition of Pt/TiO_2, Fe/TiO_2 and TiO_2 catalysts promoted the oxidation of I towards the production of organic acids with higher rate constants (k_3, k_4, k_5), while the oxidation of chloroacetic acid and acetic acid to CO_2 and formic acid remained at low levels.

4. Conclusions

In this study, was investigated the photochemical/photocatalytic oxidation of 1,3-dichloro-2-propanol aqueous solutions using hydrogen peroxide, UV irradiation and TiO_2-based catalysts enriched with platinum, cerium and iron. A reaction scheme was developed for the oxidation of 1,3-dichloro-2-propanol comprising of seven reactions: the degradation of 1,3-DCP to the chlorinated intermediate I, the degradation of I to chloroacetic, acetic and formic acids as well as towards carbon dioxide, and finally the oxidation of chloroacetic acid and acetic acid to formic acid and carbon dioxide. The oxidation efficiency of the three TiO_2-based catalysts was investigated using as criteria the 1,3-DCP conversion, the TOC removal and their effect on the reaction scheme followed during the oxidation. It was deduced that the addition of the catalysts did not affect the oxidation of 1,3-DCP to the chlorinated intermediate I ($k_1 \approx 2.5 \times 10^{-4}$ mol L^{-1} s^{-1}) for neither of the initial hydrogen peroxide concentrations investigated in this work, except from the case of Fe/TiO_2 for $[H_2O_2]_0 = 0.081$ M, where k_1 is remarkably lower

(0.628×10^{-4} mol L^{-1} s^{-1}). By the catalyst's addition, the direct mineralization of the chlorinated intermediate I is enhanced in comparison to the photochemical process for both H_2O_2 concentrations, increasing TOC removal. Formic acid produced during the oxidation remained resistant to further degradation, posing an obstacle to the total mineralization of 1,3-DCP. Finally, it was shown that under the experimental conditions investigated in this study the elimination of the initial compound as well as the removal of chloride was achieved making this process attractive to being employed as a primary step prior to biodegradation processes.

Acknowledgment

This work was supported by the Program for the Funding of Basic Research "Constantine Karatheodori" (P.E.B.E.-N.T.U.A.) 2007.

References

[1] F. Bastos, J. Bessa, C. Pacheco, P. De Marco, P.M.L. Castro, M. Silva, R. Ferreira Jorge, Biodegradation 13 (2002) 211–220.
[2] W. Chung, K. Hui, S. Cheng, J. Chromatogr. A 952 (1–2) (2002) 185–192.
[3] M.D. Nikolaki, D. Malamis, S.G. Poulopoulos, C.J. Philippopoulos, J. Hazard. Mater. 137 (2) (2006) 1189–1196.
[4] M.D. Nikolaki, C.J. Philippopoulos, J. Hazard. Mater. 146 (3) (2007) 674–679.
[5] A.M. Fauzi, D.J. Hardman, A.T. Bul, Appl. Microbiol. Biotechnol. 46 (1996) 660–666.
[6] L.B.M. Ellis, B.K. Hou, W. Kang, L.P. Wackett, Nucleic Acids Res. 31 (2003) 262–265.
[7] A. Natarajan, Y. Quian, S. Stephens, 1,3-dcp pathway map. http://umbbd.ahc.umn.edu/dcp/dcp_map.html.
[8] N. L'Huillier, M.K. Pratten, R.H. Clothier, Toxicol. In Vitro 16 (2002) 433–442.
[9] A.H. Hammond, M.J. Garle, J.R. Fry, Environ. Toxicol. Pharmacol. I (1996) 39–43.
[10] 1,3-Dichloro-2-propanol—Review of Toxicological Literature http://ntp-server.niehs.nih.gov/ntp/htdocs/Chem_Background/ExSumPdf/dichloropropanol.pdf.
[11] S. Parsons, Advanced Oxidation Processes for Water and Wastewater Treatment, IWA Publishing, UK, 2004.
[12] I.T. Peternel, N. Koprivanac, A.M. Lončarić Božić, H.M. Kušić, J. Hazard. Mater. 148 (3) (2007) 477–484.
[13] M.A. Behnajady, N. Modirshahla, N. Daneshvar, M. Rabbani, J. Hazard. Mater. 140 (1–2) (2007) 257–263.
[14] M. Muruganandham, N. Shobana, M. Swaminathan, J. Mol. Catal. A: Chem. 246 (1–2) (2006) 154–161.
[15] Q. Yang, H. Choi, Y. Chen, D.D. Dionysiou, Appl. Catal. B: Environ. 77 (3–4) (2008) 300–307.
[16] N. Serpone, J. Martin, S. Horikoschi, H. Hidaka, J. Photochem. Photobiol. A: Chem. 170 (2005) 51–60.
[17] Y. Chen, D.D. Dionysiou, Appl. Catal. A: Gen. 317 (2007) 129–137.
[18] D.D. Dionysiou, M.T. Suidan, I. Baudin, J.M. Laîné, Appl. Catal. B: Environ. 50 (2004) 259–269.
[19] T.C. Long, N. Saleh, R.D. Tilton, G.V. Lowry, B. Veronesi, Environ. Sci. Technol. 40 (14) (2006) 4346–4352.
[20] T.A. Egerton, J.A. Mattinson, J. Photochem. Photobiol. A: Chem. 194 (2–3) (2008) 283–289.
[21] T. Tong, J. Zhang, B. Tian, F. Chen, D. He, M. Anpo, J. Colloid Interf. Sci. 315 (1) (2007) 382–388.
[22] H. Měšťánková, G. Mailhot, J. Jirkovsky, J. Krysa, M. Bolte, Appl. Catal. B: Environ. 57 (4) (2005) 257–265.
[23] J.A. Wang, X. Bokhimi, O. Novaro, T. Lopez, F. Tzompantzi, R. Gomez, J. Navarrete, M.E. Lianos, E. Lopez-Salinas, J. Mol. Catal. A: Chem. 137 (1999) 239–252.
[24] R.A. Larson, E.J. Weber, Reaction Mechanisms in Environmental Organic Chemistry, Lewis Publishers, Boca Raton, FL, 1994.
[25] G. Strukul, Catalytic Oxidations with Hydrogen Peroxide as Oxidant, Kluwer Academic Publishers, Dordrecht, Netherlands, 1992.
[26] Y.J. An, S.W. Jeong, E.R. Carraway, Water Res. 35 (2001) 3276–3279.
[27] J.J. Pignatello, Environ. Sci. Technol. 26 (1992) 944–951.
[28] J.J. Pignatello, L.Q. Huang, Water Res. 27 (1993) 1731–1736.
[29] A.V. Emeline, V.K. Ryabchuk, N. Serpone, Catal. Today 122 (2007) 91–100.
[30] A.V. Emeline, V.K. Ryabchuk, N. Serpone, J. Photochem. Photobiol. A: Chem. 133 (2000) 89–97.
[31] A.G. Carlton, B.J. Turpin, K.E. Altieri, S. Seitzinger, A. Reff, H.-J. Lim, B. Ervens, Atmosp. Environ. 41 (2007) 7588–7602.
[32] I. Ilisz, K. Föglein, A. Dombi, J. Mol. Catal. A: Chem. 135 (1) (1998) 55–61.
[33] C. Adán, J.M. Coronado, R. Bellod, J. Soria, H. Yamaoka, Appl. Catal. A: Gen. 303 (2) (2006) 199–206.
[34] J. De Laat, T. Giang Le, Appl. Catal. B: Environ. 66 (2006) 137–146.
[35] E. Lipczynska-Kochany, G. Sprah, S. Harms, Chemosphere 30 (1995) 9–20.
[36] B.G. Kwon, D.S. Lee, N. Kang, J. Yoon, Water Res. 33 (1999) 2110–2118.
[37] W.Z. Tang, C.P. Huang, Environ. Technol. 17 (1996) 1371–1378.
[38] M.-C. Lu, J.-N. Chen, C.-P. Chang, Chemosphere 35 (1997) 2285–2293.
[39] J. Kiwi, A. Lopez, V. Nadtochenko, Environ. Sci. Technol. 34 (2000) 2162–2168.
[40] P.K. Malik, S.K. Saha, Sep. Purif. Technol. 31 (2003) 241–250.
[41] R. Aplin, T.D. Waite, Water Sci. Technol. 42 (2000) 345–354.
[42] J. De Laat, G.T. Le, B. Legube, Chemosphere 55 (2004) 715–723.
[43] R. Maciel, G.L. Sant'Anna Jr., M. Dezotti, Chemosphere 57 (2004) 711–719.
[44] M.-C. Lu, Y.-F. Chang, I.-M. Chen, Y.-Y. Huang, J. Environ. Manage. 75 (2005) 177–182.
[45] J. Araña, O. González Díaz, M. Miranda Saracho, J.M. Doña Rodríguez, J.A. Herrera Melián, J. Pérez Peña, Appl. Catal. B: Environ. 36 (2) (2002) 113–124.
[46] G.P. Anipsitakis, D.D. Dionysiou, M.A. Gonzalez, Environ. Sci. Technol. 40 (3) (2006) 1000–1007.
[47] W.Z. Tang, C.P. Huang, Chemosphere 33 (8) (1996) 1621–1635.